MAGMA (2004) 16: 277–283
DOI 10.1007/s10334-004-0036-x

RESEARCH ARTICLE

K. S. Weih
W. Driesel
M. von Mengershausen
D. G. Norris

Online motion correction for diffusion-weighted segmented-EPI and FLASH imaging

Received: 9 September 2003
Accepted: 23 January 2004
Published online: 29 March 2004

K. S. Weih · W. Driesel
M. von Mengershausen · D. G. Norris
Max-Planck-Institute of Cognitive Neuroscience, Stephanstr. 1a,
D-04103 Leipzig, Germany

Present address: D. G. Norris (✉)
FC Donders Centre for Cognitive Neuroimaging, Trigon,
Adelbertusplein 1, 6525 EK Nijmegen,
The Netherlands
E-mail: David.Norris@FCDonders.kun.nl
Tel.: +31-24-3610649
Fax: +31-24-3610652

Abstract This paper explores the application of online motion correction using navigator echoes to the segmented-EPI and FLASH techniques. In segmented EPI this has the advantage over post-acquisition correction that the position in k-space of each segment is no longer subject to arbitrary shifts caused by rotation. In diffusion-weighted FLASH it has the advantage that the full magnetisation can be utilised in comparison to other methods of eliminating the sensitivity to bulk motion, in which the sensitivity is halved. Healthy subjects were investigated on a 3 T whole-body system in which the hardware has been modified so that navigator echoes can be recorded on a personal computer which generates the necessary magnetic field gradient correction pulses and shifts in the Larmor frequency within 800 μs. ECG triggering was used to avoid the period of non-rigid-body brain motion. Two orthogonal navigator echoes were employed. For segmented EPI it was found essential to minimise the T2* weighting of the navigator echoes to about 10 ms to obtain reliable results. High quality images were obtained for both methods examined. Online motion correction brings direct benefits to both the diffusion-weighted segmented-EPI and FLASH techniques.

Keywords Diffusion magnetic resonance imaging · Online motion correction · Navigator echoes · Echo-planar imaging · TurboFLASH

Introduction

Diffusion-weighted imaging and diffusion tensor imaging (DWI, DTI) are both important MRI techniques with applications in the fields of clinical medicine [1-8], as well as both basic and cognitive neuroscience [9-11]. All diffusion-weighted MR experiments rely on the application of magnetic field gradients to obtain information on diffusion, the most commonly used approach being that developed by Stejskal and Tanner [12] and often known as the pulsed-gradient spin-echo, or PGSE experiment. Irrespective of the details of the diffusion sensitisation method chosen, a consequence of diffusion sensitisation is that the imaging experiment is made sensitive to small molecular displacements on the order of micrometres. Bulk motion of the object during the diffusion sensitisation period hence represents a significant measurement difficulty. Coherent motion of a group of spin isochromats during the diffusion sensitisation period will result in a phase change in the magnetisation. If the motion of the object is that of a rigid body then the movement can be described in terms of a rotation and a translation [13]. The latter will result in a phase shift whereas rotation will result in a phase gradient across the object. Single-shot imaging methods that are insensitive to the phase of the magnetisation, such as EPI, are capable of acquiring diffusion-sensitised images that have a low sensitivity to artefacts irrespective of the nature of the motion. Most

other imaging sequences have to rely however on some form of correction procedure, one of the most popular of which has proven to be that of navigator echoes [14, 15]. The use of navigator echoes to correct phase changes caused by bulk motion relies on the assumption of rigid body motion. Consequently the number of soft tissue organs for which this approach is valid is limited, but it can be applied to the brain, except for the period immediately post-systole when arterial pulsation results in the propagation of a compressive wave, which in the human can result in displacements of about 0.5 mm [16]. The effects of bulk motion on diffusion imaging and standard methods for its correction have been reviewed [17]. A more recent development is that of online navigator correction as distinct from the post-acquisition phase correction of image data on the basis of information obtained from navigator echoes [18]. Online navigator correction opens up new possibilities for correcting bulk motion in diffusion imaging of the brain. For the FLASH [19] and RARE/FSE [20] sequences it offers a potential doubling in sensitivity in comparison to methods that make these sequences insensitive to the phase of the magnetisation [21–23]. For segmented EPI it makes it possible to collect the image data equidistantly in k-space. We have previously demonstrated the value of online correction in combination with diffusion-weighted RARE imaging [18]. The purpose of this article is to describe the specific application of online correction to diffusion-sensitised segmented-EPI and FLASH sequences.

Segmented EPI is a useful adjunct to single-shot EPI as it can ameliorate some of the problems commonly encountered with the latter: viz. image distortion and limited spatial resolution. However, segmenting the acquisition increases the experimental duration, and, more pertinently, imposes the requirement of phase conformity between segments. Motion correction using 2D navigators and phase correction post-acquisition has previously been demonstrated to produce good results in humans [24–26]. In this approach the effects of rotation, which produce a shift in the k-space data, are corrected by placing the data points at the k-space coordinates corresponding to the combined effects of rotation and phase encoding, and then re-gridding to a Cartesian matrix prior to image reconstruction. Given the arbitrary nature of the variation in rotation between segments, the likelihood exists that in some images the Nyquist sampling theorem will not be satisfied. Online motion correction offers a potential solution to this problem by entirely eliminating the shift in k-space caused by rotation.

The FLASH sequence is of interest because it offers the possibility of good spatial resolution combined with low RF power requirements: qualities which become increasingly important with the move to ever higher main magnetic field strengths. As is well known, magnetisation-prepared FLASH sequences [27] read out a small percentage of the longitudinal magnetisation with each excitation. Diffusion sensitisation can hence only be achieved by bringing the bulk magnetisation into the transverse plane, applying diffusion encoding and then returning it to the longitudinal axis. Various methods of performing this have been described in the literature [28, 29]. Those that are insensitive to bulk motion all lose half the potential sensitivity either by the use of stimulated echoes [30–33] or by applying an additional dephasing gradient pulse prior to the generation of longitudinal magnetisation [21].

Methods and results

All experiments were performed using a Bruker 3 T/100 Medspec system equipped with magnetic field gradients capable of switching 45 mT m^{-1} within 320 μs. A birdcage resonator of 280 mm i.d. was used for RF-transmission and signal reception. The MPIL software package, specifically designed to drive this console, was used in all experiments. All in vivo experiments were performed on healthy adult human volunteers who had previously given informed consent to the investigation. ECG triggering was conducted using the Bruker Maglife system, so that in both sequences considered, acquisition was triggered to start 380 ms after each R-wave.

Online navigator correction was achieved by modifying the system hardware as described previously [18]. Briefly, the incoming MR signal was additionally acquired by an additional analogue to digital converter mounted in a high performance, real-time data acquisition processor board (DAP 5200a, Microstar Laboratories Inc., WA, USA) hosted by a personal computer. Echo phases and time shifts were calculated relative to a reference echo acquired without diffusion weighting. With this configuration it it possible to digitise the navigator echoes and then to output correction pulses within 800 μs of completing data acquisition. The total time required for both navigator pulses including the necessary dephase gradients was less than 6 ms. Phase gradients within the object were corrected for by applying the appropriate magnetic field gradient pulse via the console electronics. The zeroth-order phase correction was achieved by applying a pulse to the B_0-coil.

Segmented EPI

The pulse sequence employed was a standard diffusion-weighted spin-echo EPI using conventional Stejskal-Tanner spin preparation. The segments were acquired in k-space in an interleaved manner. Abrupt modulations in the k-space intensity were avoided by temporally shifting the acquisition of each k-space segment. Insertion of two perpendicular navigators plus the time necessary for any correction pulses necessary, introduces an additional delay of 8 ms. All navigator correction was performed relative to a data set acquired with minimal diffusion weighting ($b_0 = 20\,s\,mm^{-2}$). The minimum TE was 85 ms with the diffusion sensitisation taking durations of $\Delta = 40$ ms and $\delta = 22$ ms using standard notation. The sequence is sketched in Fig. 1, and was initially tested on phantoms and then on human subjects, for b-values up to $800\,s\,mm^{-2}$. One difficulty encountered in going from a phantom having a good main field homogeneity to the human head was that the T2* in vivo is considerably shorter. If the centre of the EPI echo train coincides with the centre of the spin echo then the navigator is separated from the spin-echo centre by half the echo train length (ETL) of the EPI sequence, and may hence acquire a T2* weighting corresponding to some tens of milliseconds. At 3 T it was commonly found that the

form of the gradient echo was so distorted by T2* effects that our relatively simple algorithm for finding the peak of the signal [18] no longer functioned reliably. A more complex algorithm could solve these problems, but would require more extensive computation, and may unacceptably prolong the total echo time. Hence the navigator echoes were brought as close as possible to the centre of the spin echo, without compromising image quality. In order to do this the number of segments was slightly increased and the echo train shifted so that the spin-echo maximum occurred after 30% of the total duration rather than the standard 50%, and coincided with the zero phase-encoding step. It was hence possible to acquire images on a data matrix of 128 × 128 using eight segments with an ETL of 10.24 ms. A FOV of 192 mm and a 5-mm slice thickness were used combined with a 200 kHz EPI acquisition bandwidth. With this choice of parameters the T2* weighting for the first navigator could be kept under 10 ms. In this configuration k-space shifts of about one element, and phase rotations of any angle could be successfully corrected. Images were acquired in transaxial section with diffusion weighting along the three main axes. The readout direction was along the *x*-axis. Two orthogonal navigator echoes were employed, the first navigator acquired a phase projection across the head in the readout direction, and the second acquired a projection in the phase-encoding direction. The phase information of these navigators was used to calculate correction pulses for zeroth-order and first-order phase correction [18]. This approach works best when diffusion weighting is along the slice-selection axis. However, other combinations of diffusion-weighting gradient direction and head-rotation axis can cause phase variations along the slice-selection direction that are not corrected by this configuration of orthogonal navigators. Linear phase variations along the slice-selection axis can in principle result in signal loss, but, since the slice thickness is small, the phase variation across the slice produces only a small signal attenuation, which in this instance could be neglected. A navigator echo was only used for correction, provided that its amplitude was greater than twice the mean noise level, otherwise the data were discarded. Three volunteers were measured and all gave similar results. Typical results from one measurement are shown in Fig. 2, diffusion-weighted images at maximum *b*-value of 800 s mm^{-2} (top) and corresponding ADC maps (bottom) for diffusion weighting along the three main axes are shown on the left. The isotropic diffusion-weighted image and corresponding average ADC trace (ADC_{av}) are shown on the right (fourth column). The ADC_{av} image is obtained from the average ADC value obtained from the three orthogonal directions, the DWI_{av} is obtained from the geometric mean of three DWI images with the same *b*-value but orthogonal diffusion-weighting orientations. Diffusion-sensitising gradients were applied in the readout direction in the first column, in the phase-encoding direction in the second column, and in the slice-selection direction in the third column. The anisotropy effects in the white matter regions are clearly depicted for the three different directions of diffusion-weighting gradients. Measurements with five different *b*-values (20, 215, 410, 615, 800 s mm^{-2}) were used for calculating ADC maps, the ADC_{av} map is the average of the three individual ADC maps. Some values extracted from such maps are documented in Table 1, which documents the ADC values from the volunteer shown in Fig. 2, as well as the standard deviation for the pixel values within the chosen region of interest.

FLASH

In the centric-reordered, refocussed Turbo-FLASH experiments a DEFT-variant of the Stejskal-Tanner sequence was used to generate longitudinal diffusion-weighted magnetisation. This sequence is sensitive to the effects of bulk motion because any phase change in the transverse magnetisation prior to the last 90° pulse in the DEFT sequence will strongly affect the efficiency with which diffusion-weighted magnetisation is returned to the longitudinal axis. As for the segmented-EPI experiment, two orthogonal navigators were inserted into the pulse sequence before this 90° pulse so that the phase of the magnetisation and any phase gradient could be corrected. The diffusion-weighted FLASH sequence with online motion correction is sketched in Fig. 3. In comparison with the EPI experiment somewhat shorter echo times for the diffusion-weighted preparation experiment of 62 ms could

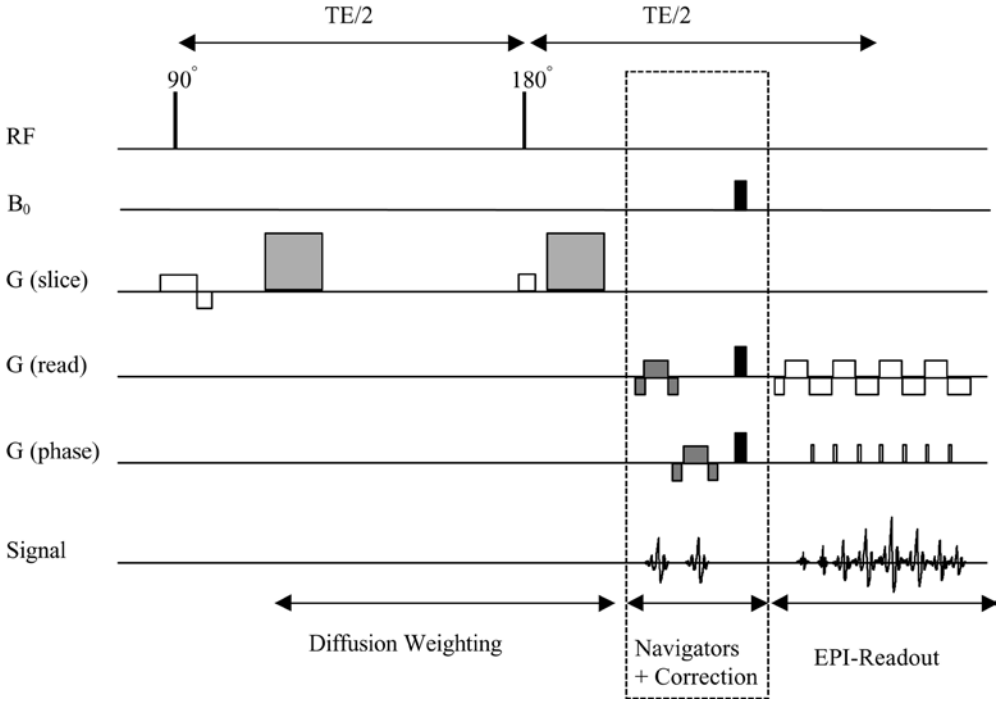

Fig. 1 Diffusion-weighted EPI sequence with online motion correction (not to scale). The diffusion weighting is performed using conventional Stejskal-Tanner spin preparation (the diffusion gradients are shaded *light grey*). In this application the diffusion weighting is in the slice-selection direction. The navigator echoes are applied in the read and phase directions, the gradient pulses required for the navigator echoes are shaded grey, the correction pulses are shaded black. The full number of phase-encoding steps employed is not shown in the schematic of the EPI readout

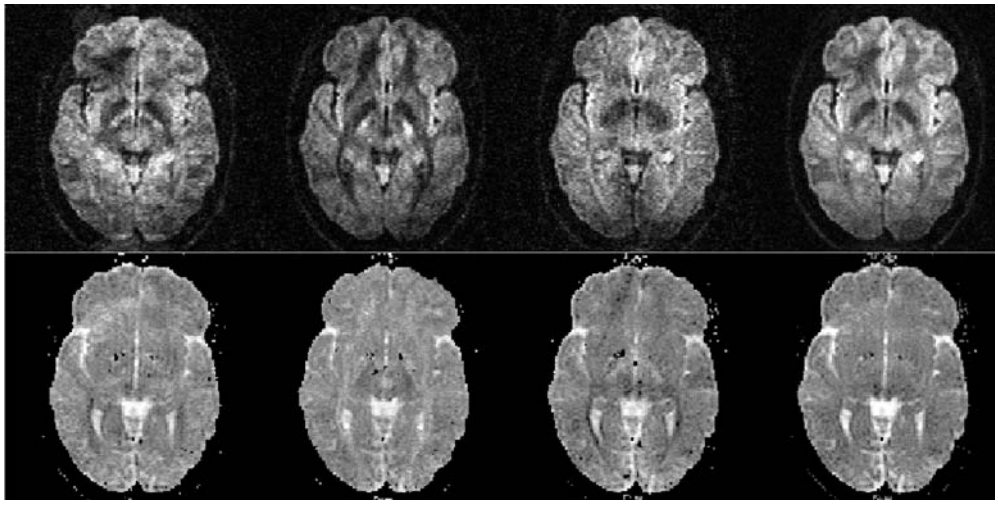

Fig. 2 Typical results obtained for diffusion-weighted segmented EPI with online motion correction for one selected slice, diffusion-weighted images with $b = 800\,\mathrm{s\,mm^{-2}}$ (*top*) and corresponding ADC maps (*bottom*). Images for diffusion weighting along the three main axes are shown on the left. Diffusion-sensitising gradients were applied in the readout direction in the first column, in the phase-encoding direction in the second column, and in the slice-selection direction in the third column. The orientation isotropic diffusion-weighted image and average ADC map (ADC_{av}) are shown at the right (forth column). For details of the acquisition parameters see text

Table 1 Mean ADC values (ADC_{aver}) for diffusion-weighted segmented EPI with online motion correction

Region of interest	ADC_{aver} (10^{-9} m^2 s^{-1})	SD (10^{-9} m^2 s^{-1})
Subcortical white matter	0.68	0.23
Corpus callosum	0.69	0.25
Putamen	0.82	0.18
Caudate nucleus, head	0.91	0.21
CSF	3.30	0.50

be achieved. FLASH images were obtained from a single preparation experiment with a data matrix of 92 (phase) × 128 (read) elements on a FOV of $184 \times 256\,\mathrm{mm^2}$, giving an in-plane resolution of 2 mm. A slice thickness of 6 mm was employed. Images were acquired in transaxial section with diffusion weighting along the slice-selection axis. Other important parameters for the FLASH sequence were α/TE/TR of 20°/3.0 ms/7.5 ms respectively. Images for ten different b-values between 20 to $800\,\mathrm{s\,mm^{-2}}$ were acquired. No averaging was performed. All imaging experiments were ECG triggered to start 380 ms post R-wave. The ADC values were calculated by performing a nonlinear least-squares fit on a pixel-by-pixel basis of the signal intensity $S(b)$ against b-values to the expression

$$S(b) = A\exp(-bADC) + B. \quad (1)$$

The diffusion-independent term B in Eq. (1) originates from the longitudinal relaxation during the relatively long FLASH readout period. For a region of interest in the splenium of the corpus callosum a value of $0.34 \pm 0.2 \times 10^{-9}\,\mathrm{m^2\,s^{-1}}$ was obtained, which is consistent with measurements to be found in the literature [34, 35].

Figure 4 shows typical images obtained with and without online motion correction obtained in transverse section from the head of a healthy human volunteer with a b-value of $800\,\mathrm{s\,mm^{-2}}$. The expected improvement in image quality is clearly demonstrated. The dark banding artefacts are almost fully removed by the online motion correction. Slight artefacts in the periventricular and brainstem region are presumably caused by non-rigid-body motion in this region that are uncorrectable by the motion correction algorithm. The clear depiction of larger blood vessels is also noteworthy. The signal from these vessels arises because of inflow during the relatively long FLASH readout train. In diffusion-weighted FLASH sequences in which the FLASH-readout portion of the sequence is modified, for example by the insertion of an additional gradient pulse [21], only the coherence pathway that has experienced the diffusion-weighted preparation experiment will be imaged. In the sequence presented here such a selection is not possible.

Discussion

The requirement to perform ECG triggering in conjunction with navigator echo correction leads inevitably to longer measurement times. In ungated segmented EPI it would generally be possible to acquire a segment from about 8 different slices per second using the parameters described above. A more aggressive strategy than that pursued in the present work would imply that data acquired during the period from 100 to 300 ms post R-wave would not be used, probably by collecting data at a constant repetition time and immediately discarding data obtained from this period. This would prolong experimental durations by about 30% as compared to an ungated experiment, but it is also to be expected that the image quality would be significantly improved for some regions of the brain. This is because even single-shot diffusion-weighted EPI can be affected by motion artefacts in ungated mode, particularly in the inferior part of the brain [36, 37]. In the FLASH sequence it takes about 800 ms to acquire data from a single slice,

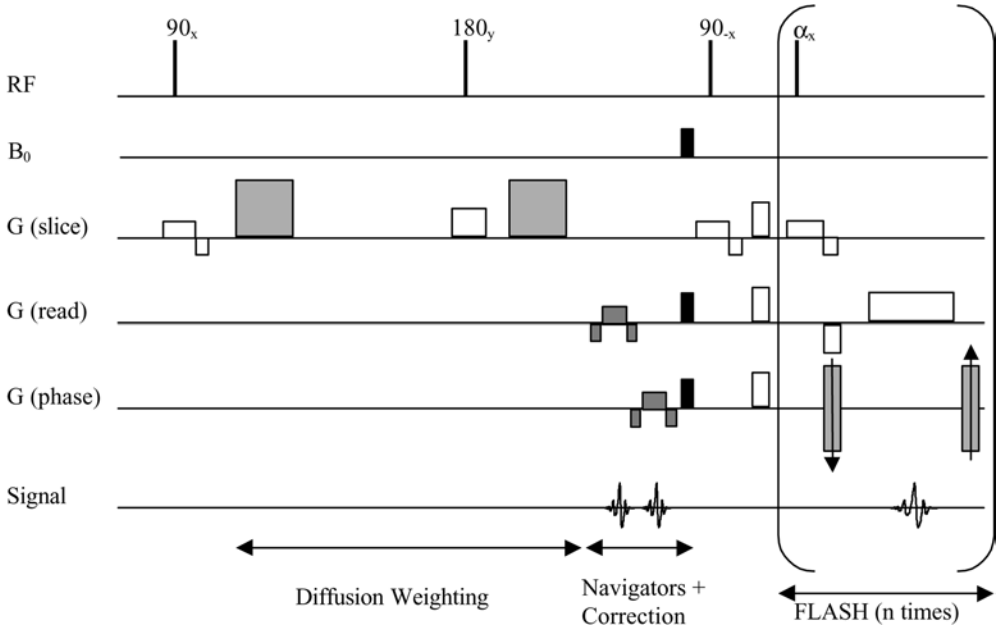

Fig. 3 Diffusion-weighted FLASH sequence with online motion correction (not to scale). The diffusion weighting is performed using conventional Stejskal-Tanner spin preparation, the diffusion-weighting gradients (shaded light *grey*) were applied in the slice-selection direction. The navigator echoes were applied in the readout and phase-encoding directions, the gradient pulses required for the navigator echoes are shaded *grey*, and the correction pulses are shaded *black*. Spoiler gradients are applied along all three axis after the magnetisation preparation period to dephase any transverse magnetisation

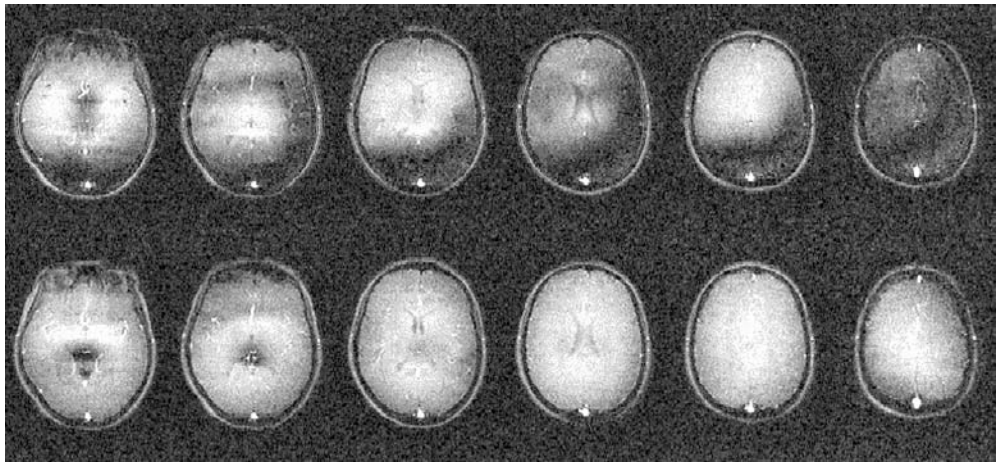

Fig. 4 Images for diffusion-weighted FLASH ($b = 800\,\mathrm{s\,mm^{-2}}$) without online motion correction (*top*), and with online motion correction (*bottom*) for a multi-slice acquisition. The improvement obtained with motion correction is clearly visible. There are flow artefacts in the region of larger vessels that result from inflow during the relatively long FLASH-readout portion of the sequence. For details of the acquisition parameters see text

whereby only the diffusion-sensitising part of the sequence should be timed so as to avoid periods of significant brain movement. In the situation where a multi-slice experiment is performed, and hence the period between acquisitions from any given slice is so long that slight variations in TR can be neglected, the loss in efficiency due to ECG triggering will be about the same as for segmented EPI. The attainment of such high levels of efficiency will however imply relatively complex sequence programming.

The standard arguments for employing segmented EPI are that it allows a reduction in the echo train length, hence reducing the degree of distortion artefacts, while allowing higher spatial resolution. In the recent past it has also become possible to attain these goals by means of parallel imaging methods [38, 39]. However, the maximum acceleration factor that can be attained in parallel imaging is limited by theoretical considerations to not more than four [40]. If the goal is to achieve a data matrix of 256×256, then at 1.5 T this may well be realisable using parallel imaging techniques, but at 3 T a factor of four will generally be insufficient. With the FLASH sequence the benefits of parallel imaging will be a reduction in the experimental duration and a possible increase in the flip angle, without a fundamental influence on the level of artefact caused by diffusion weighting.

In conclusion, this paper has successfully demonstrated that online motion correction can be successfully applied to correct rigid body bulk motion during the diffusion sensitisation period in both the segmented-EPI

and the FLASH sequences. This methodology opens the way to high spatial resolution acquisition, and improves the sensitivity of the diffusion-weighted FLASH sequence by a factor of two in comparison to other methods of desensitising this sequence to bulk motion [21, 31–33].

Acknowledgements Financial support by the University of Leipzig, Department of Neurology is gratefully acknowledged. The authors thank Manfred Weder for technical assistance with hardware modifications to the NMR system, and Reiner Hertwig for support with EPI reconstruction routines. We also thank Dr. C. Wiggings for a template segmented-EPI sequence.

References

1. Warach S, Chien D, Li W, Ronthal M, Edelman RR (1992) Fast magnetic resonance diffusion-weighted imaging of acute human stroke. Neurology 42:1717–1723
2. Warach S, Gaa J, Siewert B, Wielopolski P, Edelman RR (1995) Acute human stroke studied by whole brain echo planar diffusion-weighted magnetic resonance imaging. Ann Neurol 37:231–241
3. Chien D, Kwong KK, Gress DR, Buonanno FS, Buxton RB, Rosen BR (1992) MR diffusion imaging of cerebral infarction in humans. Am J Neuroradiol 13:1097–1102
4. Wieshmann UC, Clark CA, Symms MR, Franconi F, Barker GJ, Shorvon SD (1999) Reduced anisotropy of water diffusion in structural cerebral abnormalities demonstrated with diffusion tensor imaging. Magn Reson Imaging 17:1269–1274
5. Maier CF, Paran Y, Bendel P, Rutt BK, Degani H (1997) Quantitative diffusion imaging in implanted human breast tumors. Magn Reson Med 37:576–581
6. Lim KO, Hedehus M, Moseley M, de Crespigny A, Sullivan EV, Pfefferbaum A (1999) Compromised white matter tract integrity in schizophrenia inferred from diffusion tensor imaging. Arch Gen Psychiatry 56:367–374
7. Horsfield MA, Larsson HB, Jones DK, Gass A (1998) Diffusion magnetic resonance imaging in multiple sclerosis. J Neurol, Neurosurg &Psychiatr 64(Suppl 1):S80–S84
8. Hugg JW, Butterworth EJ, Kuzniecky RI (1999) Diffusion mapping applied to medial temporal lobe epilepsy: preliminary observations. Neurology 53:173–176
9. Jones DK, Simmons A, Williams SC, Horsfield MA (1999) Non-invasive assessment of axonal fiber connectivity in the human brain via diffusion tensor MRI. Magn Reson Med 42:37–41
10. Mori S, Kaufmann WE, Davatzikos C, Stieltjes B, Amodei L, Fredericksen K, Pearlson GD, Melhem ER, Solaiyappan M, Raymond GV, Moser HW, van Zijl PC (2002) Imaging cortical association tracts in the human brain using diffusion-tensor-based axonal tracking. Magn Reson Med 47:215–223
11. Conturo TE, Lori NF, Cull TS, Akbudak E, Snyder AZ, Shimony JS, McKinstry RC, Burton H, Raichle ME (1999) Tracking neuronal fiber pathways in the living human brain. Proc Natl Acad Sci USA 96:10,422–10,427
12. Stejskal EO, Tanner JE (1965) Spin diffusion measurements: spin echoes in the presence of a time-dependent field gradient. J Chem Phys 42:288–292
13. Anderson AW, Gore JC (1994) Analysis and correction of motion artifacts in diffusion weighted imaging. Magn Reson Med 32:379–387
14. Ehman RL, Felmlee JP (1989) Adaptive technique for high-definition MR imaging of moving structures. Radiology 173:255–263
15. Ordidge RJ, Helpern JA, Qing ZX, Knight RA, Nagesh V (1994) Correction of motional artifacts in diffusion-weighted MR images using navigator echoes. Magn Reson Imaging 12:455–460
16. Greitz D, Wirestam R, Franck A, Nordell B, Thomsen C, Stahlberg F (1992) Pulsatile brain movement and associated hydrodynamics studied by magnetic resonance phase imaging. the Monro-Kellie doctrine revisited. Neuroradiology 34:370–380
17. Norris DG (2001) Implications of bulk motion for diffusion-weighted imaging experiments: effects, mechanisms, and solutions. J Magn Reson Imaging 13:486–495
18. Norris DG, Driesel W (2001) Online motion correction for diffusion-weighted imaging using navigator echoes: application to RARE imaging without sensitivity loss. Magn Reson Med 45:729–733
19. Haase A, Frahm J, Matthaei D, Hänicke W, Merboldt K-D (1986) FLASH imaging. rapid NMR imaging using low flip-angle pulses. J Magn Reson 67:258–266
20. Hennig J, Nauerth A, Friedburg H (1986) RARE imaging: a fast imaging method for clinical MR. Magn Reson Med 3:823–833
21. Sinha U, Sinha S (1996) High speed diffusion imaging in the presence of eddy currents. J Magn Reson Imag 6:657–666
22. Norris DG, Börnert P, Reese T, Leibfritz D (1992) On the application of ultra-fast RARE experiments. Magn Reson Med 27:142–164
23. Alsop DC (1997) Phase insensitive preparation of single-shot RARE: application to diffusion imaging in humans. Magn Reson Med 38:527–533
24. Butts K, de Crespigney A, Pauly JM, Moseley M (1996) Diffusion-weighting interleaved echo-planar imaging with a pair of orthogonal navigator echoes. Magn Reson Med 35:763–770
25. Butts K, Pauly J, de Crespigny A, Moseley M (1997) Isotropic diffusion-weighted and spiral-navigated interleaved EPI for routine imaging of acute stroke. Magn Reson Med 38:741–749
26. Atkinson D, Porter DA, Hill DL, Calamante F, Connelly A (2000) Sampling and reconstruction effects due to motion in diffusion-weighted interleaved echo planar imaging. Magn Reson Med 44:101–109
27. Haase A (1990) Snapshot FLASH MRI. Applications to T1, T2, and chemicalshift imaging. Magn Reson Med 13:77–89
28. Deimling M, Mueller E, Laub G (1990) Diffusion weighted imaging with turbo-FLASH. In: Proceedings: 9th annual meeting of the society of magnetic resonance in medicine, p 387
29. Lee H, Price RR (1994) Diffusion imaging with the MP-RAGE sequence. J Magn Reson Imaging 4:837–842
30. Merboldt KD, Hanicke W, Bruhn H, Gyngell ML, Frahm J (1992) Diffusion imaging of the human brain in vivo using high-speed STEAM MRI. Magn Reson Med 23:179–192

31. Merboldt KD, Hanicke W, Frahm J (1991) Diffusion imaging using stimulated echoes. Magn Reson Med 19:233–239
32. Yongbi MN, Ding S, Dunn JF (1996) A modified sub-second fast-STEAM sequence incorporating bipolar gradients for in vivo diffusion imaging. Magn Reson Med 35:911–916
33. Nolte UG, Finsterbusch J, Frahm J (2000) Rapid isotropic diffusion mapping without susceptibility artifacts: whole brain studies using diffusion-weighted single-shot STEAM MR imaging. Magn Reson Med 44:731–736
34. Hanyu H, Asano T, Sakurai H, Imon Y, Iwamoto T, Takasaki M, Shindo H, Abe K (1999) Diffusion-weighted and magnetization transfer imaging of the corpus callosum in Alzheimer's disease. J Neurol Sci 167:37–44
35. Abe O, Aoki S, Hayashi N, Yamada H, Kunimatsu A, Mori H, Yoshikawa T, Okubo T, Ohtomo K (2002) Normal aging in the central nervous system: quantitative MR diffusion-tensor analysis. Neurobiol Aging 23:433–441
36. Brockstedt S, Borg M, Geijer B, Wirestam R, Thomsen C, Holtas S, Stahlberg F (1999) Triggering in quantitative diffusion imaging with single-shot EPI. Acta Radiologica 40:263–269
37. Skare S, Andersson JLR (2001) On the effects of gating in diffusion imaging of the brain using single shot EPI. Magn Reson Imaging 19:1125–1128
38. Sodickson DK, Manning WJ (1997) Simultaneous acquisition of spatial harmonics (SMASH): fast imaging with radiofrequency coil arrays. Magn Reson Med 38:591–603
39. Pruessmann KP, Weiger M, Scheidegger MB, Boesiger P (1999) SENSE: sensitivity encoding for fast MRI. Magn Reson Med 42:952–962
40. Wiesinger F, Pruessmann KP, Boesiger P (2002) Potential and limitations of parallel imaging at high field strength. MAGMA 15:447